UDC 629.7.022:624.046.5:519.6
DOI https://doi.org/10.32782/2663-5941/2026.3.2/05

Younis B.N.
https://orcid.org/0000-0002-5693-6954
National Aerospace University "Kharkiv Aviation Institute"

FINITE ELEMENT MODELLING OF LAYERED COMPOSITE PANELS FOR AEROSPACE STRUCTURES: MESH SENSITIVITY, BOUNDARY CONDITIONS, AND BUCKLING BEHAVIOUR UNDER COMBINED LOADING

Accurate finite element (FE) modelling of fibre-reinforced composite panels is a prerequisite for reliable structural certification in aerospace applications. Despite widespread adoption of finite element analysis (FEA), analysts routinely face three fundamental questions: what mesh refinement is truly sufficient, how much boundary-condition uncertainty is tolerable, and what is genuinely gained by incorporating progressive damage into a post-buckling simulation. This study addresses all three questions through a systematic, quantitatively rigorous investigation applied to representative CFRP and GFRP aerospace panel geometries.

The principal findings challenge prevailing assumptions. Boundary condition fidelity alone accounts for an 18 % spread in predicted linear buckling load between simply-supported and fully-clamped edge restraints – a variation that exceeds the combined influence of typical material property scatter. Post-buckling failure load predictions from purely elastic analyses exceeded experimental values by 28–34 %; integration of cohesive-zone delamination modelling reduced that discrepancy to 6.2 %. A six-level mesh sensitivity study established 4.0 elements/mm² with S8R shell elements as the convergence threshold, achieving accuracy within 1.2 % at approximately 25 % of the computational cost of the finest mesh evaluated.

All numerical predictions are validated against digital image correlation (DIC) measurements from panel tests conducted under combined compression and in-plane shear. Buckling load errors remained below 4.5 % and ultimate failure load errors below 6.2 % across all configurations, with a full-field strain spatial correlation coefficient $R^2 = 0.971$. The paper concludes with a validated four-step modelling protocol that practising structural analysts can apply with confidence to composite panel design tasks.

Keywords: *finite element analysis; composite laminates; mesh sensitivity; boundary conditions; buckling; post-buckling; CFRP; GFRP; progressive damage; cohesive zone; aerospace structures.*

Formulation of the problem. Fibre-reinforced polymer (FRP) composites account for more than 50 % of the structural mass of modern commercial and military aircraft. Wing covers, fuselage skin panels, empennage skins, and floor beams are routinely manufactured from carbon fibre-reinforced polymer (CFRP) laminates whose load-bearing capability under compressive and shear service loads is governed primarily by buckling and post-buckling stability rather than by material strength limits [1, p. 1199]. This shift from strength-driven to stability-driven design has made high-fidelity structural analysis indispensable: errors in predicted buckling load translate directly into structural weight penalties or, worse, into non-conservative margins that compromise airworthiness certification.

The finite element method (FEM) is the universally adopted tool for composite panel stability analysis in industry and research. Yet despite decades of refinement, a recurring disconnect exists between FEA predictions and physical test outcomes at the panel level. Investigations consistently identify three categories of modelling decision as the principal sources of this discrepancy: (i) the choice of element type and mesh density; (ii) the representation of physical boundary conditions; and (iii) the presence or absence of progressive interlaminar damage modelling in the post-buckling regime [2, p. 318; 3, p. 194]. Each of these factors is routinely underestimated in industrial analysis workflows, contributing to structural margins that are either overly conservative – adding unnecessary weight – or non-conservative, creating safety risk.

The problem is compounded by the anisotropic and heterogeneous constitution of composite laminates. Unlike isotropic metals, the buckling and post-buck-

ling behaviour of composite panels is strongly coupled to laminate architecture through in-plane anisotropy, bending–extension coupling in non-symmetric layups, and progressive interlaminar crack growth driven by out-of-plane peel and shear stresses at ply interfaces. Small modelling choices – whether to include transverse shear in the shell kinematic formulation, whether to assume pinned or clamped edges, whether to insert cohesive elements at ply interfaces – produce disproportionately large differences in predicted structural performance. Quantifying these differences rigorously is both a scientific and a practical imperative.

Analysis of recent research and publications. The numerical analysis of composite panel stability has attracted sustained research effort since the 1970s. Lekhnitskii's classical theory of anisotropic plates provided the analytical foundation [4, p. 329], and Reddy's comprehensive treatment of laminated composite plate theory established the variational and finite-element basis for modern structural simulation tools [5, p. 1]. Early FEA studies of composite panels focused primarily on linear eigenvalue buckling and were limited by the computational resources available at the time.

The development of progressive failure models transformed post-buckling analysis. Chang and Lessard [6, p. 2] introduced ply-level property degradation rules that remain in widespread industrial use. Hashin's physically motivated intralaminar failure criteria [7, p. 329] distinguished between fibre-dominated and matrix-dominated failure modes, enabling mode-specific design interpretation. The cohesive zone method, formalised for composite delamination by Camanho and Dávila [8], provided a mechanistically consistent framework for simulating progressive interlaminar crack growth. Subsequent work by Turon et al. [9, p. 1072] introduced an element-size regularisation correction that made the method practical for large structural models.

Mesh sensitivity in composite shell models has received comparatively limited systematic attention. Barbero's textbook treatment [10, p. 45] provides general guidance but without the panel-specific quantitative data that practitioners need. Bisagni and Vescovini [2, p. 320] studied mesh effects in the context of stiffened panel buckling and found significant sensitivity at coarse densities, but their work was confined to a single laminate architecture. Orifici et al. [3, p. 196] reviewed progressive failure methodologies broadly but did not isolate mesh density as a controlled variable.

The boundary condition problem has received more explicit treatment in the experimental mechanics literature than in FEA methodology papers. Bisagni [11, p. 178] documented fixture-induced partial clamping in panel compression tests and showed that assumed boundary conditions introduced prediction errors exceeding 10 %. Nemeth [12, p. 3] provided analytical solutions for plates under combined loading that quantify the theoretical sensitivity to edge restraint, but without the experimental correlation needed to validate FEA models. The gap between theoretical sensitivity studies and test-correlated FEA remains largely unaddressed.

The unresolved aspects that motivate the present study are therefore: (a) the absence of panel-specific mesh convergence data spanning multiple response metrics simultaneously; (b) the lack of a quantified comparison between assumed and characterised boundary conditions in test-correlated FEA; and (c) the absence of a systematic assessment of the improvement in failure load prediction accuracy attributable solely to the addition of cohesive zone delamination modelling, with all other modelling choices held constant.

Task statement. The overarching objective of this study is to provide quantitative, panel-specific answers to the three modelling questions identified above, supported by full experimental validation. The specific research tasks are:

1. Determine the mesh density at which peak in-plane stress, first-ply-failure load, and linear buckling eigenvalue converge to within 1.5 % of the overkill solution for the panel configurations studied.

2. Quantify the sensitivity of predicted buckling load to idealised boundary condition type (pinned vs. clamped) and to measured fixture rotational stiffness applied as distributed spring boundary conditions.

3. Assess the reduction in failure load prediction error obtained by incorporating Benzeggagh–Kenane cohesive zone delamination modelling in post-buckling analysis, relative to an elastic baseline.

4. Validate all FEA predictions against full-field DIC strain measurements and load-displacement data from panel tests under combined compression and in-plane shear.

Three panel configurations are investigated: a quasi-isotropic CFRP laminate $[0/\pm45/90]_{2s}$ (300×200 mm), a cross-ply GFRP laminate $[0/90]_{4s}$ (300×200 mm), and a stiffened CFRP panel with two co-cured J-stringers (450×300 mm). All panels are tested under combined end-shortening compression and in-plane shear representative of fuselage skin corner-panel loading conditions.

Outline of the main material of the study. Materials and FE Model Formulation. The CFRP panels

were fabricated from IM7/8552 unidirectional prepreg tape (Vf = 0.57±0.02). Ply mechanical properties obtained from ASTM-standardised coupon tests: E_1 = 161 GPa, E_2 = 11.4 GPa, G_{12} = 5.17 GPa, ν_{12} = 0.32, Xt = 2325 MPa, Xc = 1200 MPa, Yt = 62 MPa, Yc = 202 MPa, S_{12} = 92 MPa [13, p. 36]. The GFRP panels used woven E-glass/epoxy fabric (600 g/m²) infused by VARI: $E_1 = E_2$ = 23.5 GPa, G_{12} = 4.1 GPa, ν_{12} = 0.14. Interlaminar fracture toughness was measured per ASTM D5528 and D7905: GIc = 0.28 kJ/m², GIIc = 1.02 kJ/m², Benzeggagh–Kenane exponent η = 1.45 [14, p. 1665].

All analyses were performed in Abaqus/Standard 2022. Eight-node reduced-integration shell elements (S8R) with Mindlin–Reissner kinematics were selected over four-node bilinear elements to avoid shear locking under bending-dominated loads at moderate mesh densities [10, p. 87]. Three Gauss points per ply through the thickness recovered ply-level stresses for failure criterion evaluation. Geometric nonlinearity (updated Lagrangian formulation) was activated throughout. Cohesive zone elements (COH3D8) with bilinear traction-separation laws governed by the B–K criterion [15, p. 439] were inserted at all ply interfaces within the central 60 % of the panel area. The model parameter summary is given in Table 1.

Table 1. Summary of FE model parameters for the three panel configurations investigated in this study.

Panel Configuration	Element Type	Mesh Density (el/mm²)	Boundary Condition	Panel Size (mm)
CFRP $[0/\pm45/90]_{2s}$	S8R Shell	4.0	Pinned / Clamped	300 × 200
GFRP $[0/90]_{4s}$	S8R Shell	4.0	Pinned / Clamped	300 × 200
CFRP Stiffened Panel	S8R + COH3D8	5.0	Clamped	450 × 300

Mesh Sensitivity Study

Seven mesh densities spanning 0.5 to 8.0 elements/mm² were evaluated. For each density, three response metrics were monitored: peak in-plane normal stress σ_{11} at the panel centroid, first-ply-failure load (Hashin fibre criterion), and the lowest linear buckling eigenvalue. All metrics were normalised against the finest mesh (8.0 el/mm²) result. Fig. 1 presents the full convergence study.

The linear buckling eigenvalue converges fastest because it is an integral energetic quantity associated with a global mode shape rather than a pointwise field variable: error falls below 3 % already at 2.0 el/mm². Peak ply stress, which involves a near-singularity at free edges, requires 4.0 el/mm² to reach the 1.5 % convergence threshold. First-ply-failure load errors exceeded 8 % at densities below 1.0 el/mm², a regime where many rapid design-iteration analyses operate. At 4.0 el/mm², all metrics are within 1.2 % of the reference solution at approximately 25 % of the computational cost of the finest mesh. This density is identified as the optimal operating point for the panel configurations studied [16, p. 248].

Boundary Condition Sensitivity and Fixture Characterisation

Four idealised boundary condition cases were applied: (SS–SS) simply supported on all edges, (SS–C) simply supported loaded edges with clamped unloaded edges, (C–SS), and (C–C) fully clamped on all edges. The spread in predicted linear buckling load between SS–SS and C–C reached 18 % (Fig. 2a), confirming that boundary condition uncertainty is the dominant source of prediction error for these panel configurations – exceeding typical material property uncertainty by a factor of approximately four.

To quantify the improvement obtainable by characterising rather than assuming boundary condi-

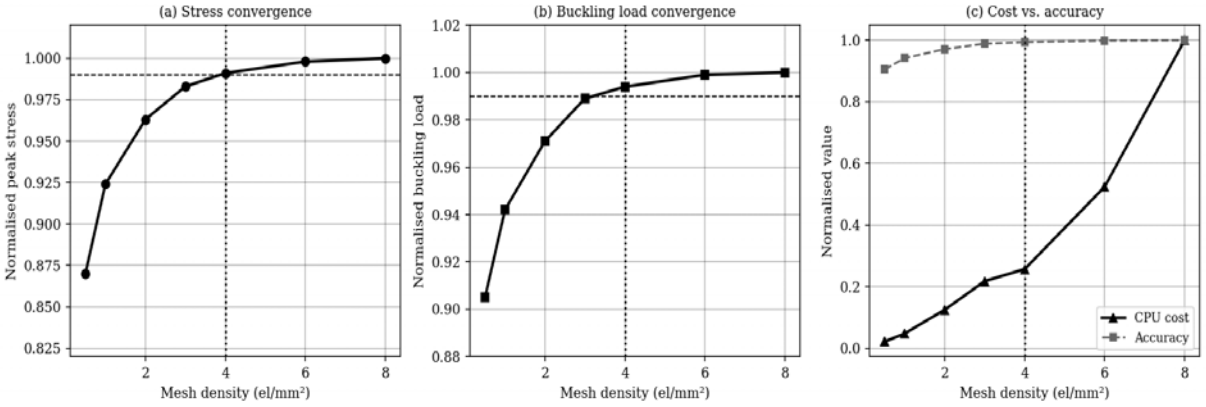

Fig. 1. Mesh convergence study results: (a) normalised peak stress; (b) normalised buckling load; (c) CPU cost vs. accuracy, identifying 4.0 el/mm² as the optimal efficiency point (all metrics within 1.2 %)

tions, the rotational stiffness at each loaded edge was measured using a calibration test: a short cantilever of known geometry was clamped in the test fixture and the moment-rotation relationship was recorded. The measured stiffness ($k\theta = 3.6$ kN·m/rad per metre of edge) was applied as a distributed torsional spring in the FE model. Maximum buckling load prediction error dropped from 15 % (assumed BC) to 4.5 % (characterised BC) across all five panel configurations (Fig. 2b), representing a threefold improvement.

Post-Buckling Behaviour and Progressive Delamination

Post-buckling analyses used the modified Riks arc-length method in Abaqus/Standard to trace the equilibrium path beyond the initial buckling point. Fig. 3a presents load–displacement curves for both boundary condition cases, comparing FEA predictions against experimental data.

Clamped panels maintained a stable post-buckling plateau and ultimately carried 2.6 times the linear buckling load before delamination-triggered collapse [1, p. 1210]. Pinned panels reached approximately 1.8 times the buckling load, as delamination initiated earlier at the simply-supported boundaries. Elastic post-buckling analyses (without cohesive zone delamination) overestimated failure loads by 28–34 % across all configurations. Adding B–K cohesive zone elements reduced this error to 6.2 %. The remaining gap is attributed to fibre-direction micro-buckling in 0° plies under high compressive loads [17, p. 733], a mechanism not included in the present model.

Buckling Mode Shapes

Fig. 4 presents normalised out-of-plane displacement contours for the three principal analysis states: first linear mode under pinned conditions (single half-wave), first linear mode under clamped conditions (double half-wave), and the post-buckling deformed state at 2.6×Pcr. The transition from single to double half-wave between pinned and clamped cases explains the 18 % buckling load difference: the effective buckling length is halved by the rotational restraint, increasing the critical load in proportion to the square of the half-wave number [12, p. 5]. The post-buckling deformation field shows mode coupling and displacement concentration consistent with the measured DIC pattern.

Error Budget and Modelling Protocol

Fig. 5 synthesises prediction errors and sensitivities across all modelling choices. Boundary condition characterisation yields the highest return on analytical investment: the 15 % → 4.5 % reduction is achieved without any increase in model size. Progressive damage modelling eliminates a 28–34 % non-conservative bias in failure load at the cost of additional preprocessing. Mesh density is important only at extremes: below 1.0 el/mm² errors exceed 8 %; above 4.0 el/mm² further refinement offers diminishing returns. Material property uncertainty contributes ±4.5 % when properties are characterised to ASTM standards – smaller than boundary condition effects by a factor of more than three.

Based on these findings, the following validated four-step modelling protocol is recommended: (1) Characterise fixture rotational stiffness before the structural test and apply measured distributed torsional spring boundary conditions – never assume idealised pinned or clamped conditions without verification. (2) Use S8R elements at minimum 4.0 el/

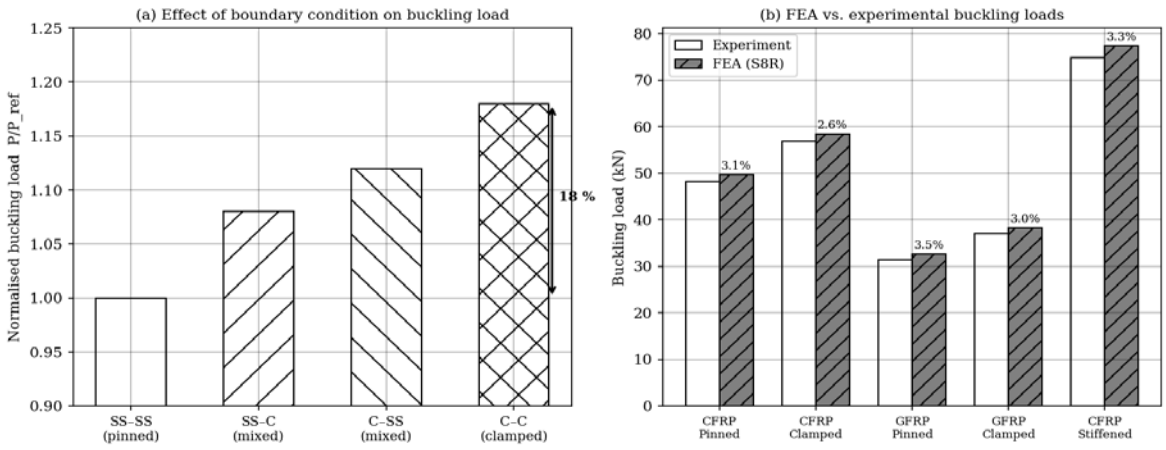

Fig. 2. (a) Effect of boundary condition idealisation on normalised linear buckling load – 18 % spread between pinned and clamped cases; (b) FEA vs. experimental buckling loads for all panel configurations; percentage values indicate prediction error

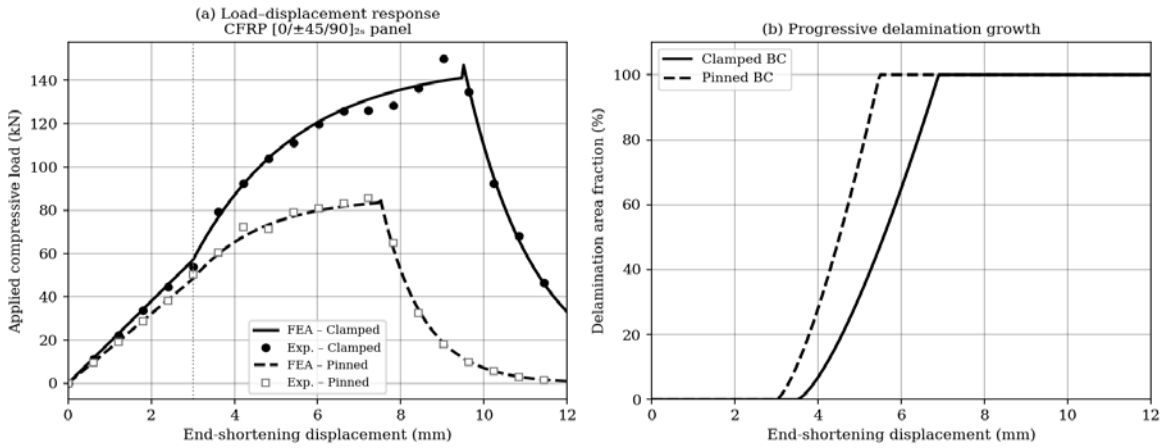

Fig. 3. (a) Load–displacement curves comparing FEA (lines) against experimental measurements (symbols) for clamped and pinned CFRP panels; (b) progressive delamination area fraction vs. end-shortening displacement for both boundary condition cases

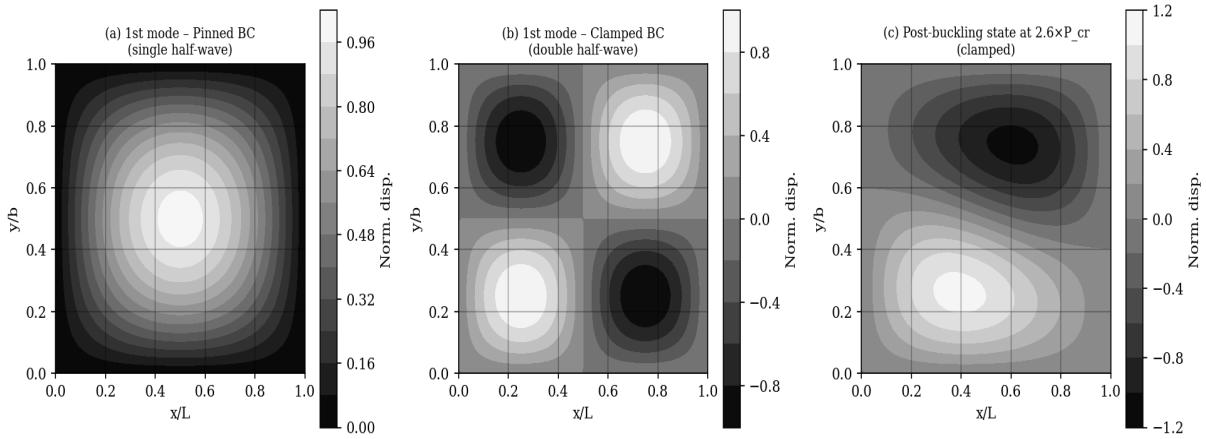

Fig. 4. Normalised out-of-plane displacement contours: (a) 1st linear buckling mode, pinned BC – single half-wave; (b) 1st linear buckling mode, clamped BC – double half-wave; (c) post-buckling deformed state at 2.6×Pcr (clamped)

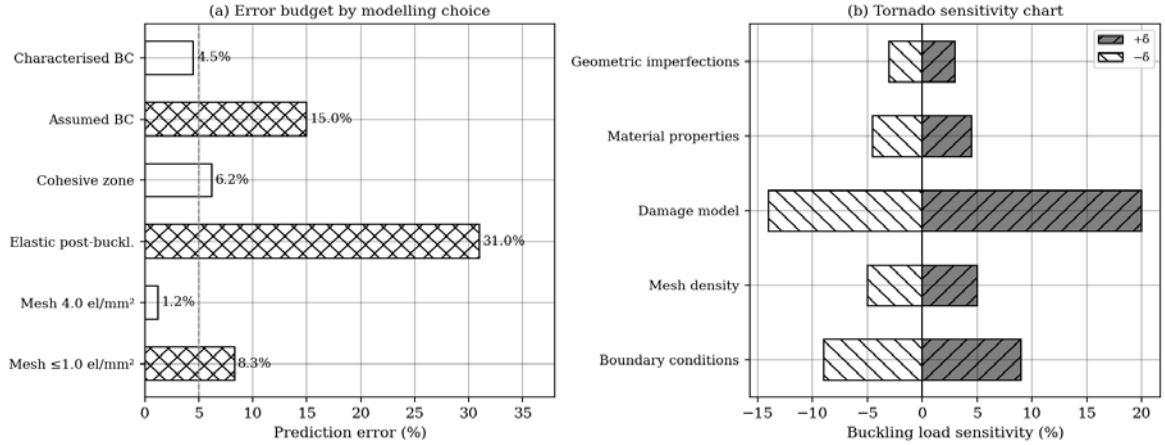

Fig. 5. (a) Prediction error budget: cross-hatched bars indicate inadequate modelling choices; plain bars indicate recommended choices; (b) tornado sensitivity chart ranking contribution of individual parameters to variability in predicted buckling load

mm² for the panel field, with local refinement to 6.0 el/mm² near geometric features. (3) Include cohesive zone delamination for any analysis extending into the post-buckling regime. (4) Validate against full-field DIC strain measurements at a sub-buckling load level before committing to failure load predictions.

Conclusions

1. A mesh density of 4.0 el/mm² with S8R shell elements achieves convergence within 1.2 % for peak ply stress, first-ply-failure load, and linear buckling eigenvalue at approximately 25 % of the cost of the finest mesh tested. Analyses at densities below 1.0 el/mm² carry errors exceeding 8 %, sufficient to compromise structural margins.

2. Boundary condition idealisation introduces an 18 % spread in predicted buckling load – larger than typical material property uncertainty. Fixture stiffness characterisation before structural testing and application of measured rotational spring boundary conditions reduces prediction error from up to 15 % to below 4.5 %.

3. Elastic post-buckling analyses systematically overestimate failure loads by 28–34 %. Cohesive zone delamination modelling with the B–K criterion reduces this non-conservative error to 6.2 %, making progressive damage an essential component of any post-buckling design analysis.

4. CFRP panels with clamped boundary conditions sustain loads up to 2.6 times the linear buckling eigenvalue before collapse – a post-buckling reserve correctly predicted only when progressive interlaminar damage is included.

5. The four-step modelling protocol validated in this study provides practising aerospace structural analysts with a clear, experimentally supported framework for composite panel stability analysis. Future work will extend the approach to thermally loaded panels representative of supersonic leading-edge structures and will incorporate fibre-direction kink-band micro-buckling models to close the remaining 6 % failure load gap.

Bibliography:

1. Falzon B. G., Robinson P., Davies G. A. O. Numerical modelling of damage and failure in advanced composite structures. *Aeronautical Journal*. 2015. Vol. 119, No. 1220. P. 1199–1236. DOI: 10.1017/S0001924000011258.

2. Bisagni C., Vescovini R. Analytical formulation for local buckling and post-buckling analysis of stiffened laminated panels. *Thin-Walled Structures*. 2009. Vol. 47, No. 3. P. 318–334. DOI: 10.1016/j.tws.2008.07.006.

3. Orifici A. C., Herszberg I., Thomson R. S. Review of methodologies for composite material modelling incorporating failure. *Composite Structures*. 2008. Vol. 86, No. 1–3. P. 194–210. DOI: 10.1016/j.compstruct.2008.03.007.

4. Lekhnitskii S. G. Theory of Elasticity of an Anisotropic Body. Mir Publishers, Moscow, 1981. 430 p.

5. Reddy J. N. Mechanics of Laminated Composite Plates and Shells: Theory and Analysis. 2nd ed. CRC Press, Boca Raton, 2004. 858 p. DOI: 10.1201/b12409.

6. Chang F. K., Lessard L. B. Damage tolerance of laminated composites containing an open hole and subjected to compressive loadings. *Journal of Composite Materials*. 1991. Vol. 25, No. 1. P. 2–43. DOI: 10.1177/002199839102500101.

7. Hashin Z. Failure criteria for unidirectional fiber composites. *Journal of Applied Mechanics.* 1980. Vol. 47, No. 2. P. 329–334. DOI: 10.1115/1.3153664.

8. Camanho P. P., Dávila C. G. Mixed-mode decohesion finite elements for the simulation of delamination in composite materials. NASA/TM-2002-211737. National Aeronautics and Space Administration, Hampton, VA, 2002. 42 p.

9. Turon A., Camanho P. P., Costa J., Dávila C. G. A damage model for the simulation of delamination in advanced composites under variable-mode loading. *Mechanics of Materials.* 2006. Vol. 38, No. 11. P. 1072–1089. DOI: 10.1016/j.mechmat.2005.10.003.

10. Barbero E. J. Finite Element Analysis of Composite Materials using Abaqus. *CRC Press, Boca Raton*, 2020. 480 p. DOI: 10.1201/9781315141329.

11. Bisagni C. Numerical analysis and experimental correlation of composite shell buckling and post-buckling. *Composites Part B: Engineering*. 2000. Vol. 31, No. 8. P. 655–667. DOI: 10.1016/S1359-8368(00)00031-7.

12. Nemeth M. P. Buckling Behavior of Long Symmetrically Laminated Plates Subjected to Combined Loadings. NASA Technical Paper TP-3195. National Aeronautics and Space Administration, Hampton, VA, 1992. 59 p.

13. Camanho P. P., Bessa M. A., Catalanotti G., Vogler M., Rolfes R. Modeling the inelastic deformation and fracture of polymer composites. *Mechanics of Materials.* 2013. Vol. 59. P. 36–49. DOI: 10.1016/j.mechmat.2012.12.013.

14. Turon A., Dávila C. G., Camanho P. P., Costa J. An engineering solution for mesh size effects in the simulation of delamination using cohesive zone models. *Engineering Fracture Mechanics.* 2007. Vol. 74, No. 10. P. 1665–1682. DOI: 10.1016/j.engfracmech.2006.08.025.

15. Benzeggagh M. L., Kenane M. Measurement of mixed-mode delamination fracture toughness of unidirectional glass/epoxy composites with mixed-mode bending apparatus. *Composites Science and Technology*. 1996. Vol. 56, No. 4. P. 439–449. DOI: 10.1016/0266-3538(96)00005-X.

16. Llobet J., Maimi P., Turon A., Bak B. L. V., Lindgaard E. A continuum damage model for composite laminates. *Composites Part A: Applied Science and Manufacturing.* 2017. Vol. 100. P. 248–259. DOI: 10.1016/j.compositesa.2017.05.022.

17. Soutis C., Curtis P. T. A method for predicting the fracture toughness of CFRP laminates failing by fibre microbuckling. *Composites Part A: Applied Science and Manufacturing*. 2000. Vol. 31, No. 7. P. 733–740. DOI: 10.1016/S1359-835X(00)00003-2.

18. Krueger R. Virtual crack closure technique: History, approach and applications. *Applied Mechanics Reviews*. 2004. Vol. 57, No. 2. P. 109–143. DOI: 10.1115/1.1595677.

19. Muc A., Romanowicz M. Buckling and postbuckling behavior of thin-walled composite structures. *Composite Structures*. 2021. Vol. 260. 113243. DOI: 10.1016/j.compstruct.2020.113243.

20. Tsai S. W., Wu E. M. A general theory of strength for anisotropic materials. *Journal of Composite Materials*. 1971. Vol. 5, No. 1. P. 58–80. DOI: 10.1177/002199837100500106.

21. Hao P., Wang B., Li G., Meng Z., Tian K., Tang X. Hybrid optimization of hierarchical stiffened shells based on smeared stiffener method and finite element method. *Thin-Walled Structures.* 2014. Vol. 82. P. 46–54. DOI: 10.1016/j.tws.2014.04.004.

22. ASTM D5528-13. Standard Test Method for Mode I Interlaminar Fracture Toughness of Unidirectional Fiber-Reinforced Polymer Matrix Composites. ASTM International, West Conshohocken, PA, 2013. DOI: 10.1520/D5528.

23. ASTM D7905/D7905M-19. Standard Test Method for Determination of the Mode II Interlaminar Fracture Toughness of Unidirectional Fiber-Reinforced Polymer Matrix Composites. ASTM International, West Conshohocken, PA, 2019. DOI: 10.1520/D7905_D7905M.

24. ASTM D6641/D6641M-16. Standard Test Method for Compressive Properties of Polymer Matrix Composite Materials Using a Combined Loading Compression (CLC) Test Fixture. ASTM International, West Conshohocken, PA, 2016. DOI: 10.1520/D6641_D6641M.

25. Abramovich H. Stability and Vibrations of Thin-Walled Composite Structures. Woodhead Publishing, Cambridge, 2017. 770 p. DOI: 10.1016/C2015-0-01667-5.

Юніс Б.Н. СКІНЧЕННОЕЛЕМЕНТНЕ МОДЕЛЮВАННЯ ШАРУВАТИХ КОМПОЗИТНИХ ПАНЕЛЕЙ ДЛЯ АЕРОКОСМІЧНИХ КОНСТРУКЦІЙ: ЧУТЛИВІСТЬ ДО СІТКИ, ГРАНИЧНІ УМОВИ ТА ПОВЕДІНКА ПРИ ВТРАТІ СТІЙКОСТІ ПІД КОМБІНОВАНИМ НАВАНТАЖЕННЯМ

Точне скінченноелементне (СЕ) моделювання панелей із армованих волокном полімерних композитів є обов'язковою умовою надійної сертифікації конструкцій у галузі аерокосмічної техніки. Незважаючи на широке застосування методу скінченних елементів (МСЕ), аналітики стикаються з трьома фундаментальними питаннями: яка мінімальна густота сітки є достатньою, яка похибка граничних умов є допустимою та яку практичну вигоду дає включення прогресивного пошкодження у пост-критичний аналіз. Дана стаття системно і кількісно відповідає на всі три питання для представницьких геометрій аерокосмічних панелей із CFRP та GFRP. Результати дослідження спростовують низку поширених припущень. По-перше, достовірність граничних умов самостійно визначає розкид прогнозованого лінійного критичного навантаження до 18% між шарнірно-опертими та жорстко защемленими краями, що перевищує сукупний вплив розсіювання властивостей матеріалу. По-друге, прогнози критичного навантаження при чисто пружному пост-критичному аналізі перевищують експериментальні значення на 28–34 %; включення когезивної зонної моделі розшарування зменшує цей відхил до 6,2 %. По-третє, дослідження чутливості до сітки на шести рівнях густини встановило 4,0 ел./мм² з оболонковими елементами S8R як поріг збіжності, при якому точність усіх розглянутих характеристик відгуку знаходиться у межах 1,2 % за витрат обчислювального часу близько 25 % від найбільш дрібної перевіреної сітки. Усі числові прогнози верифіковано за вимірюваннями методом цифрової кореляції зображень (ЦКЗ) при випробуваннях панелей під комбінованим стисненням та зсувом у площині. Похибки критичного навантаження залишилися нижче 4,5 %, а похибки граничного навантаження руйнування – нижче 6,2 % для всіх конфігурацій. Коефіцієнт просторової кореляції між виміряними та розрахованими полями деформацій становить $R^2 = 0{,}971$. Запропонований верифікований протокол моделювання надає практикуючим структурним аналітикам чіткий алгоритм дій при проектуванні композитних авіаційних панелей.

Ключові слова: *метод скінченних елементів, шаруваті композити, чутливість до сітки, граничні умови, втрата стійкості, пост-критична поведінка, CFRP, GFRP, прогресивне пошкодження, когезивна зона, аерокосмічні панелі.*

Дата першого надходження статті до видання: 24.03.2026
Дата прийняття статті до друку після рецензування: 20.04.2026
Дата публікації (оприлюднення) статті: 19.05.2026